

Modelling Dover Harbour using the LABSWE

Andrew Cunningham, Jian Zhou and Jon Shiach

School of Computing, Mathematics and Digital Technology

Manchester Metropolitan University

United Kingdom

March 2020

Abstract: Dover Harbour requires significant dredging of sediment around the harbour entrances annually. With the recent revival of the western harbour a significant portion of this sediment has been resourced to help with the construction. The majority of the sediment comes from these tidal flows from the North Sea and English Channel. The lattice Boltzmann method with shallow water equations, LABSWE, has been used to produce the tidal currents within the harbour. A dredging of 20m has been undertaken in the Outer Harbour. This dredging had small effect and further measures may be necessary to reduce this amount. We considered adding a small breakwater within the western harbour's entrance and extending the western arm creating a smaller entrance for turbulent flow which is a major contributor to sediment deposit. This had significant impact into the reduction of flow within the harbour.



Keywords: Lattice Boltzmann method, shallow water equations, Dover harbour, LABSWE

Supervisory Points:

1 Introduction

Dover Harbour, considered to be busiest passenger harbour in Europe, experiences a build-up of silt and sediment predominantly around the two main entrances. Up to $250,000\ m^3$ of mud and sand is deposited away from the harbour however due to the strong tidal currents from both the North Sea and the English Channel these areas fill up quickly. The movement of the tidal flows across the harbour exceeds the threshold shear stress of the bed causing the transport of sediment to these areas (Dey 1999). Shields (1936).

Since 2018 a revival of Dover Harbours western dock has been taken place to grant new opportunities and investment into the harbour. This change will expand the western docks and add a new area to house small vessels. The revival will use dredged material to help with the construction of the expanded areas. However once the Dover Western Dock Revival, also known as DWDR, has been completed will this new expansion change tidal flows within the harbour and potentially increase the amount to be dredged. If so can the harbour be dredged further to reduce the turbulent

waters that may enter the harbour.

Shallow seas, such as those seen in the Strait of Dover, differ from their larger, deeper counterparts due to the geostrophic acceleration, coastal boundaries, etc. acting upon them (Bowden 1956). These factors influence the tidal currents greatly. Breakwaters have a considerable impact and prevent turbulent erratic flow from entering the harbour and preventing travel. The breakwater around Dover harbour started to be built within 1847 to decrease these influences (Vernon-Harcourt 1885). The water renovation and flushing from the harbour has been studied by Sanchez-Arcilla (2002) as has the effect of having two entrances to the harbour.

The effect of both the North Sea and the English Channel give a residual circulation pattern that ebbs and flows high and low tides (Prandle et al. 1993). These tides directly affect the harbour by flowing across the top of it thus creating small inner vortices both inside and outside of the harbour. The vortices created by these two differing flows has been observed both in Dover and in Calais (Latteux 1980).

The lattice Boltzmann method, LBM, has shown promise as a modern numerical method for solving incompressible flow problems (Guo, Shi, and Wang 2000) and is a successor to the lattice gas automata, (Wolf-Gladrow 2000) which comprised of Boolean logic to determine where particles lay within a system. The role of the lattice Boltzmann method is to describe the simulation through the mesoscopic range, the bridge between the microscopic and the macroscopic worlds (McNamara and Zanetti 1988). In this range a group of particles are considered rather than mapping the complete particle interactions. Then the macroscopic quantities are developed and associated to the system, necessary for the formulation of the Navier-Stokes equations. This allows the method to be easily paralleled with other machines (Huang et al. 2015).

The shallow water equations, SWE, have been used to model a wide range of fluid flow problems from tidal flows with a good amount of accuracy (Kelly et al. 2016) to open channel flows (Peng, Zhou, and Burrows 2011). Zhou has proposed a conjunction of the nonlinear SWE with the LBM, LABSWE, for river and coastal engineering. The LABSWE has been adopted due to its efficiency and simplicity particularly when dealing with boundary conditions (Zhou 2007).

Within this paper a look into how the new revival of the Western Harbour within Dover Harbour effects the tidal flows using the LABSWE method.

2 Methodology

2.1 Governing Equations

The 2D SWE with source terms of bed slope and bed friction may be written in tensor notation as

$$\begin{aligned} \frac{\partial h}{\partial t} + \frac{\partial(hu_i)}{\partial x_i} &= 0, \\ \frac{\partial(hu_i)}{\partial t} + \frac{\partial(hu_i u_j)}{\partial x_j} &= -g \frac{\partial h^2}{\partial x_i} \frac{h^2}{2} - gh \frac{\partial z_b}{\partial x_u} - \frac{\tau_{bi}}{\rho} + \frac{\partial}{\partial x_j}(h\nu \frac{\partial u_i}{\partial x_j}) \end{aligned} \quad (1)$$

where i, j are the indices and the Einstein summation convention is used therefore if a repeated indices is used then a summation over the space coordinates. The Cartesian coordinate is x_i , h is the water depth, t is the time, u_i is the depth-averaged velocity component in the i direction, z_b

is the bed elevation, $g = 9.81 \text{ m/s}^2$ is the acceleration due to gravity, ρ is the water density, ν the kinematic viscosity, τ_{bi} the bed shear stress along the $i - th$ direction defined by

$$\tau_{bi} = \rho C_b u_i \sqrt{u_j u_j} \quad (2)$$

where C_b is the bed friction coefficient.

2.2 Lattice Boltzmann Model

The Bhatnagar, Gross Krook Method 1953, also known as the single-relaxation time method, SRT, has been modified to calculate the SWE (~~Jian Guo~~ Zhou 2011)

$$f_i(x + e_i \delta t, t + \delta t) - f_i(x, t) = \frac{1}{\tau} (f_i^{eq} - f_i) + \frac{\delta t}{6e^2} e_{ij} F_j \quad (3)$$

where f_i and f_i^{eq} is the particle distribution function and the particle equilibrium function respectively, x is the two dimensional Cartesian coordinate of space, t is the time unit, δt is the time step, e_i is the particle velocity vector described upon the lattice configuration in Figure 1 where $i = 0, \dots, 8$, e_{ij} is the particle velocity component within the j direction, $e = \delta x / \delta t$ where δx is the lattice size, and τ is the single-relaxation parameter which is related to the depth-averaged eddy viscosity ν by

$$\tau = \frac{6\nu + 1}{2}. \quad (4)$$

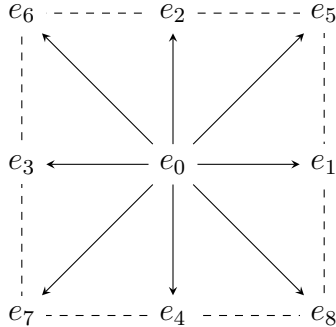


Figure 1: A two-dimensional 9 vertex lattice.

f_i^{eq} is defined as

$$f_i^{eq} = \begin{cases} h(1 - \frac{5gh}{6e^2} - \frac{2u^2}{3e^2}) & \text{if } i = 0, \\ h(\frac{gh}{6e^2} + \frac{e_i u}{3e^2} + \frac{e_i^2 u^2}{2e^4} - \frac{u^2}{6e^2}) & \text{if } i = 1, 2, 3, 4, . \\ \frac{1}{4}h(\frac{gh}{6e^2} + \frac{e_i u}{3e^2} + \frac{e_i^2 u^2}{2e^4} - \frac{u^2}{6e^2}) & \text{if } i = 5, 6, 7, 8. \end{cases} \quad (5)$$

The forcing term F_i is given by

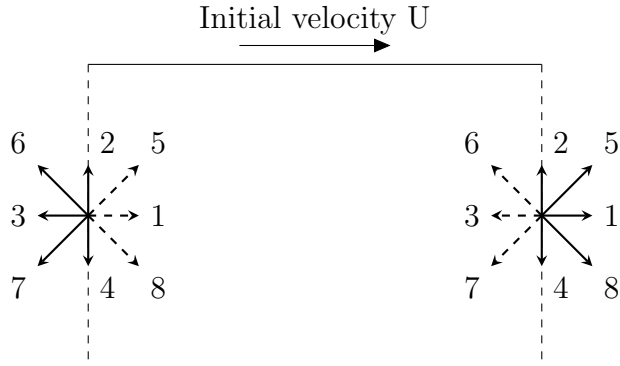


Figure 2: Example of a channel flow describing the boundary conditions

$$F_i = -gh \frac{\partial z_b}{\partial x_i} + \frac{\tau_{wi}}{\rho} - \frac{\tau_{bi}}{\rho} + \Omega h u_y \delta_{ix} - \Omega h u_x \delta_{iy}, \quad (6)$$

where h and u_i is the average water depth and the depth-averaged velocity, $g = 9.81m/s^2$ is the acceleration due to gravity, z_b is the bed elevation, τ_{wi} is the wind shear stress, τ_{bi} is the bed shear stress, ρ is the water density, Ω is the Coriolis parameter to take the Earth's rotation into effect, and δ_{ij} is the Kronecker delta function given by

$$\delta_{ij} \begin{cases} 0, & \text{if } i = j, \\ 1, & \text{if } i \neq j. \end{cases} \quad (7)$$

The macroscopic variables of both water depth and velocity are defined

$$h = \sum_{i=0}^8 f_i, \quad (8)$$

$$u = \frac{1}{h} \sum_{i=0}^8 e_i f_i \quad (9)$$

2.3 Boundary Conditions

For the current simulations a combination of both non-slip and Zou-He boundary conditions have been implemented. For the non-slip, also known as a traditional bounce-back boundary condition, the particle is reflected from a solid surface. These conditions have been used at the solid boundaries of the harbour and across the south, east and west boundaries of the cavity as seen in Figure 2. The LBM solves these conditions through

$$\begin{aligned} f_1 &= f_3, & f_2 &= f_4, \\ f_5 &= f_7, & f_6 &= f_8. \end{aligned} \quad (10)$$

A non-slip boundary condition has also been applied to the challenging harbour geometry. For this complicated geometry the last known fluid node available before colliding with the curved

boundary is used and the next known area after the collision is represented as a solid. Figure 3 represents this technique.

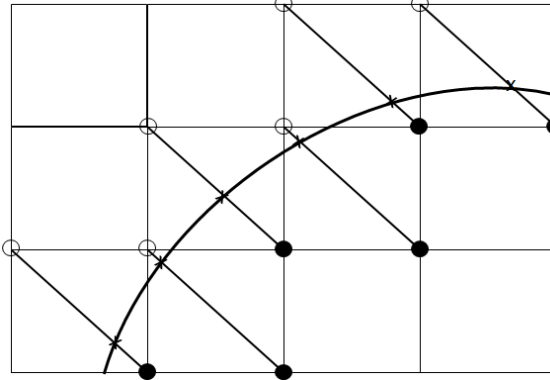


Figure 3: Layout of a regularly spaced lattice with a curved boundary. The thick curve represents the curved boundaries location. The x upon the boundary curve represents the particle collision boundary. The empty and shaded circles denote the fluid and solid nodes respectively.

Using the boundary conditions posed by [Liu, J. Zhou, and R. Burrows 2012](#), both the inlet and outlet boundary conditions can be discovered. They proposed that the boundary conditions can be found using a mass and momentum balance following the Zou-He boundary conditions (Zou and He 1997). Take the inlet on the left-handside for example, the unknown velocity vectors, e_1, e_5 and e_8 , can be extrapolated using the known vectors. Hence discovering

$$\begin{aligned} f_1 &= f_3 + \frac{2hu}{3e}, \\ f_5 &= \frac{hu}{6e} + f_7 + \frac{f_4-f_2}{2}, \\ f_8 &= \frac{hu}{6e} + f_6 + \frac{f_2-f_4}{2}. \end{aligned} \quad (11)$$

However this scheme does not fully close as both the velocity and water-depth are unknown at the inlet. [Liu, J. Zhou, and R. Burrows](#) propose two new steps that conserve both the mass and momentum of the system, these two steps are the assigning and compensation step respectively. For the assigning step a zero-gradient boundary is used at the inlet for the macroscopic variables, h, u and v . For the compensation step the discharge per unit width, hu , is converted to $(Q_{in} - Q_c)/b$. Where Q_{in} is the constant discharge, Q_c is the discharge calculated within the assigning step using h, u and v , and b is the width of the channel. Thus the new inlet boundary conditions can be defined as

$$\begin{aligned} f_1 &= f_3 + \frac{2hu}{3e}, \\ f_5 &= \frac{hu+(Q_{in}-Q_c)/b}{6e} + f_7 + \frac{f_4-f_2}{2} + \frac{hv}{2e}, \\ f_8 &= \frac{hu+(Q_{in}-Q_c)/b}{6e} + f_6 + \frac{f_2-f_4}{2} - \frac{hv}{2e}. \end{aligned} \quad (12)$$

3 Results

A 400x400 domain was created to represent the Dover Harbour space seen within ?? with an initial velocity at the inlet upon the left hand-side set to $u = 1m/s^2$. The simulations water depth was set to $h = 6m$ to represent the high water, HW, tides seen within Dover. The discharge rate was set to $Q = 2.2m/s^3$.



Figure 4: Topological map of Dover Harbour

Using satellite imagery areas of the harbour were analysed and drawn to represent the more complicated geometry of the harbour. Then using the topological data found in 4 the bed elevation can be found for a more accurate representation of the tidal flows. Using this map an approximation of the shallow and deep waters can be obtained. For simplicity the green areas are estimated to be of a higher elevation than the water depth. However using the the mean tidal profile within ?? and agreement of average depth 0.1m has been established.

The average water height has been reduced by about 1:10 to stay within the required SWE stability range. The time step $dt = 0.01$ and ran until the time step was after a 3 hour HW approximation. These simulations have all been shown at HW as this was the most turbulent time for the harbour in particular.

For the simulation seen within Figures 6 the harbour is using the topological data and the high water data. When compared to the set seen within Figure 5 many similarities become apparent. A vortex is being created outside of the harbour due to the breakwater. The outer harbour and the entrances experience a dramatic decrease in speed compared to the rest of the simulation. Small vortices are seen to be created within the southern entrance which is where the majority of the smaller vessels depart from. However within the simulation the large vortex seen within the northern entrance in 5 at both HW and an hour past does not seem to form within the LBM models. This method has dampened some of the features seen within the HR Wallingford model as within Figure 5b a vortex can be seen within the eastern harbour entrance which does not seem to be as prominent within Figure 6a.

One key area that is affected predominantly at high tides is the southern entrance. This is created by the English Channel bypassing the entrance creating vortexes at the entrance. The dredging at the entrances, seems to affect these the most. Seen within Figures 7 the southern entrance seems to create more vortices however are much more condensed compared to Figures 6. This can be seen when looking at the velocity vectors for the two cases, there seems to be more activity at the HW, Figure 8, than the LW 5.

In Figures 7 the bed in the outer harbour has been decreased by 2m along the entrances and near the breakwater creating a small channel. This has seemed to dampen the more intense vortices being created within the harbour, primarily within Figure 6b to a more manageable size seen

within Figure 7a. Also from this dredged channel more flow seemed to be diverted away from the inner harbour making it calmer for both vessels and swimmers. When looking at the figures seen within Figure 8 the slowest speeds are within the inner harbour where the depth is the lowest.

Another breakwater was added into the entrance of the western harbour entrance towards the bottom of the harbour within the simulations. This was to further reduce the amount of the turbulent flow entering from this entrance and therefore reduce the amount of sediment that could be transported with those flows. In conjunction with this a small extension was added to the western harbour entrances breakwater reducing the size of the entrance. As mostly smaller vessels use this entrance a way of limiting the amount of tumultuous waters that could effect travel.

Observing the streamlines seen within Figure 9 by extending the breakwater a significant amount of the flow that comes from the English Channel seen at the left hand bottom portion of the simulation bypasses the harbour. Looking at Figure ?? the breakwater within the Outer Harbour portion of the entrance has a significant impact upon limiting the amount of flow entering the harbour assuming for safer and easier travel to and from the new DWDR. However a turbulent vortex is created at when $t = 2$ in Figure 9e outside of the harbour. This dissipates at the later hours but could be a cause for concern for depositing sediment outside the harbour affecting travel.

4 Conclusions

The tidal flows seen within Dover Harbour have been modelled using the lattice Boltzmann method. Dredging within the harbour looks to be a short term solution at improving the overall flow within the harbour making it more accessible for vessels to travel particularly around the harbour entrances. However adding or extending the western harbour entrance with further breakwaters seems to have significant impact upon the amount of turbulent flow at HW entering the harbour which could limit the amount of deposited silt and sediment entering the harbour. Therefore a reduction in the amount needing to be dredged annually.

5 Acknowledgement

References

- Bhatnagar, P. L., E.P. Gross, and M. Krook (1953). *A Kinetic Approach to Collision Processes in Gases: Small Amplitude Processes in Charged and Neutral One Component Systems*. Tech. rep. Massachusetts: Massachusetts Institute of Technology.
- Bowden, K. F. (Feb. 1956). “The Flow of Water through the Straits of Dover, Related to Wind and Differences in Sea Level”. In: *Philosophical Transactions of the Royal Society A: Mathematical, Physical and Engineering Sciences* 248.953, pp. 517–551. ISSN: 1364-503X. DOI: 10.1098/rsta.1956.0008.
- Dey, Subhasish (1999). “Sediment threshold”. In: *Applied Mathematical Modelling*. ISSN: 0307904X. DOI: 10.1016/S0307-904X(98)10081-1.

- Guo, Zhaoli, Baochang Shi, and Nengchao Wang (2000). “Lattice BGK Model for Incompressible Navier-Stokes Equation”. In: *Article in Journal of Computational Physics* 165, pp. 288–306. DOI: 10.1006/jcph.2000.6616.
- Huang, Changsheng et al. (2015). “Multi-GPU based lattice boltzmann method for hemodynamic simulation in patient-specific cerebral aneurysm”. In: *Communications in Computational Physics*. ISSN: 19917120. DOI: 10.4208/cicp.2014.m342.
- Kelly, Samuel M et al. (2016). “A Coupled-Mode Shallow-Water Model for Tidal Analysis: Internal Tide Reflection and Refraction by the Gulf Stream”. In: *JOURNAL OF PHYSICAL OCEANOGRAPHY* 46, pp. 3661–3679. DOI: 10.1175/JPO-D-16-0018.1.
- Latteux, B. (1980). “Harbour Design Including Sedimentological Problems Using Mainly Numerical Techniques”. In: *Coastal Engineering*.
- Liu, H., J.G. Zhou, and R. Burrows (2012). “Inlet and outlet boundary conditions for the Lattice-Boltzmann modelling of shallow water flows”. In: *Progress in Computational Fluid Dynamics, An International Journal*. ISSN: 20500416. DOI: 10.1002/jib.143.
- Masters, Steve. (2019). *Mean Spring Tide Tidal Currents*. Tech. rep. Dover: Port of Dover, p. 5.
- McNamara, Guy R. and Gianluigi Zanetti (Nov. 1988). “Use of the Boltzmann Equation to Simulate Lattice-Gas Automata”. In: *Physical Review Letters* 61.20, pp. 2332–2335. ISSN: 0031-9007. DOI: 10.1103/PhysRevLett.61.2332. URL: <https://link.aps.org/doi/10.1103/PhysRevLett.61.2332>.
- Peng, Y., J G Zhou, and R Burrows (2011). “Modelling solute transport in shallow water with the lattice Boltzmann method”. In: DOI: 10.1016/j.compfluid.2011.07.008.
- Prandle, D. et al. (June 1993). “The influence of horizontal circulation on the supply and distribution of tracers”. In: *Philosophical Transactions of the Royal Society of London. Series A: Physical and Engineering Sciences* 343.1669, pp. 405–421. DOI: 10.1098/rsta.1993.0055.
- Sanchez-Arcilla, A. et al. (2002). “Water Renovation in Harbour Domains. The Role of Wave and Wind Conditions”. In: *Coastal Engineering 2002*. WORLD SCIENTIFIC. ISBN: 978-981-238-238-2.
- Shields, A and J C Van Uchelen (1936). “Application of Similarity Mechanics and Turbulence Research to Bed Load Movement”. PhD thesis. California Institute of Technology.
- Vernon-Harcourt, L.F. (1885). *Harbours and Docks*. Cambridge: Cambridge University Press, p. 650. ISBN: 978-1-108-07202-1.
- Wolf-Gladrow, Dieter A. (2000). *Lattice Gas Cellular Automata and Lattice Boltzmann Models*. ISBN: 978-3-540-66973-9. DOI: 10.1007/b72010.
- Zhou, J.G. (2007). “Comparison study of lattice Boltzmann method and Godunov method for shallow water flows”. In: *Proceedings of 32nd Congress of IAHR*, Venice.

Zhou, Jian Guo (2011). “Enhancement of the LABSWE for shallow water flows”. In: *Journal of Computational Physics*. ISSN: 00219991. DOI: [10.1016/j.jcp.2010.09.027](https://doi.org/10.1016/j.jcp.2010.09.027).

Zou, Qisu and Xiaoyi He (1997). “On pressure and velocity flow boundary conditions and bounce-back for the lattice Boltzmann BGK model”. In: *Physics of Fluids* 9.6, pp. 1591–1598. DOI: [10.1063/1.869307](https://doi.org/10.1063/1.869307).

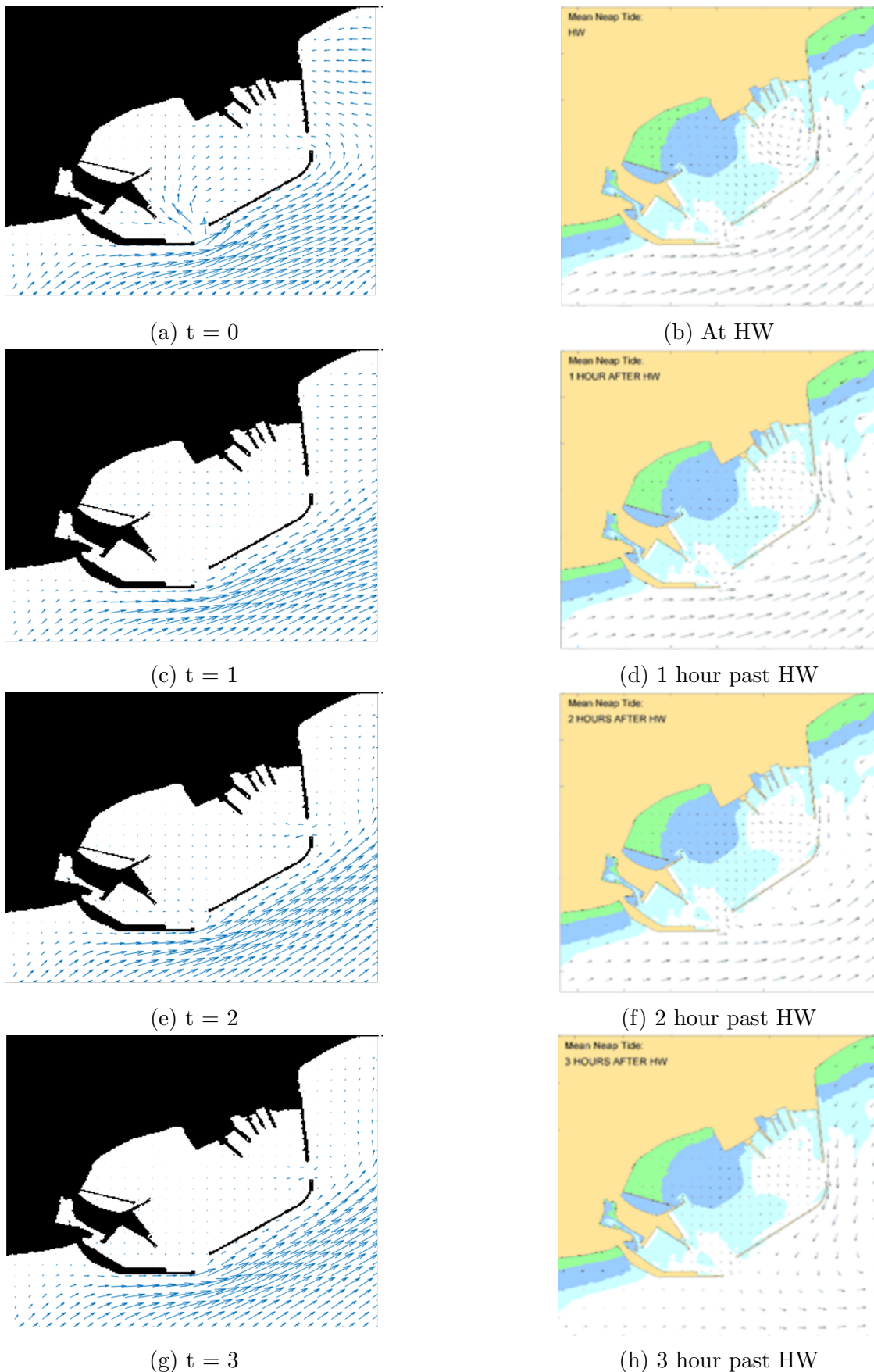


Figure 5: The velocity vector profile of the mean tidal (L) at HW compared with results from HR Wallingford (R) (Masters 2019)

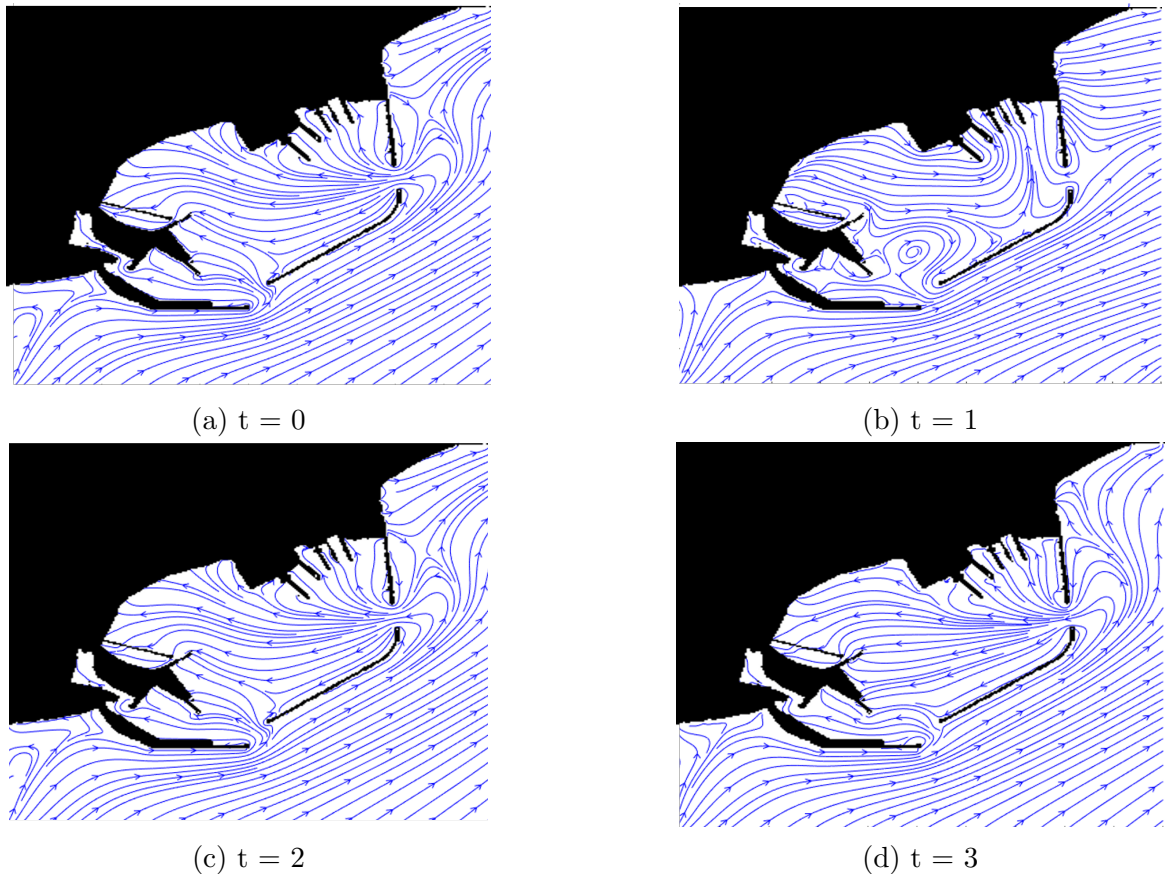
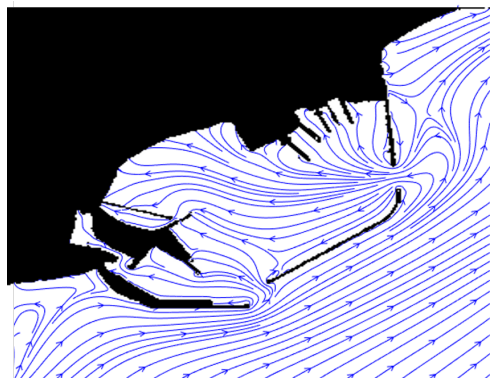
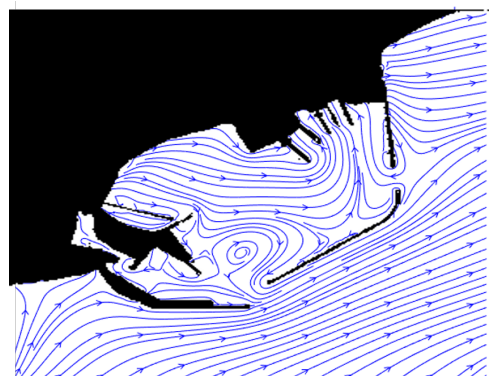


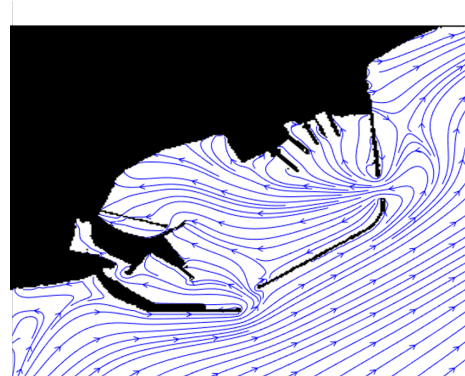
Figure 6: The mean tidal average using the lattice Boltzmann method at HW and three more consecutive hours after HW



(a) $t = 1$

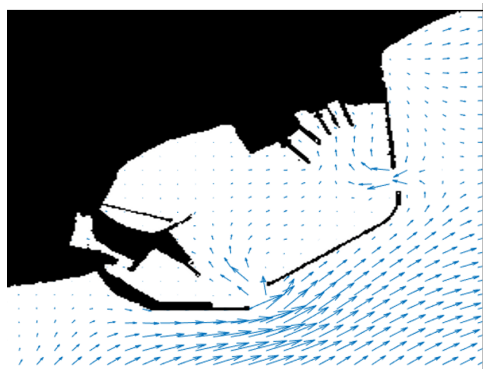


(b) $t = 2$

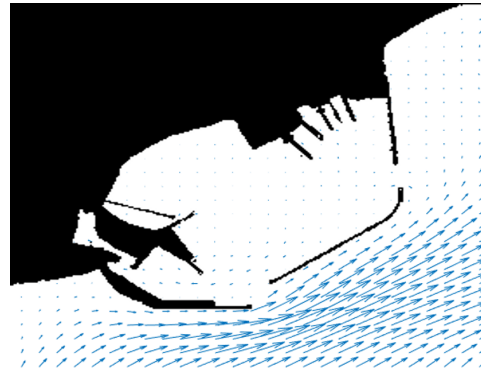


(c) $t = 3$

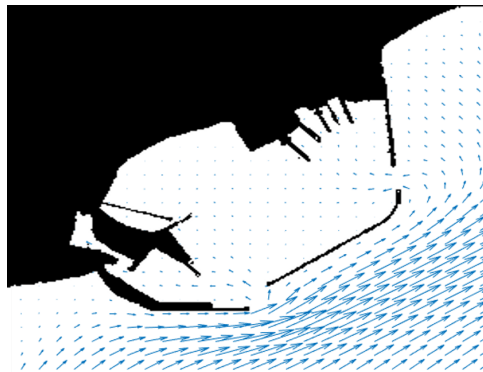
Figure 7: The mean tidal average when the outer harbour has been dredged by a further 20m



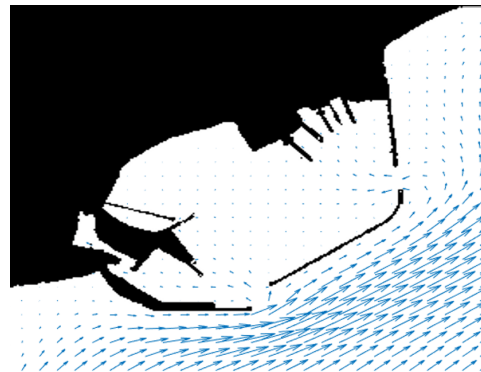
(a) $t = 0$



(b) $t = 1$



(c) $t = 2$



(d) $t = 3$

Figure 8: Mean tidal flow velocity vector after being dredged by 20m

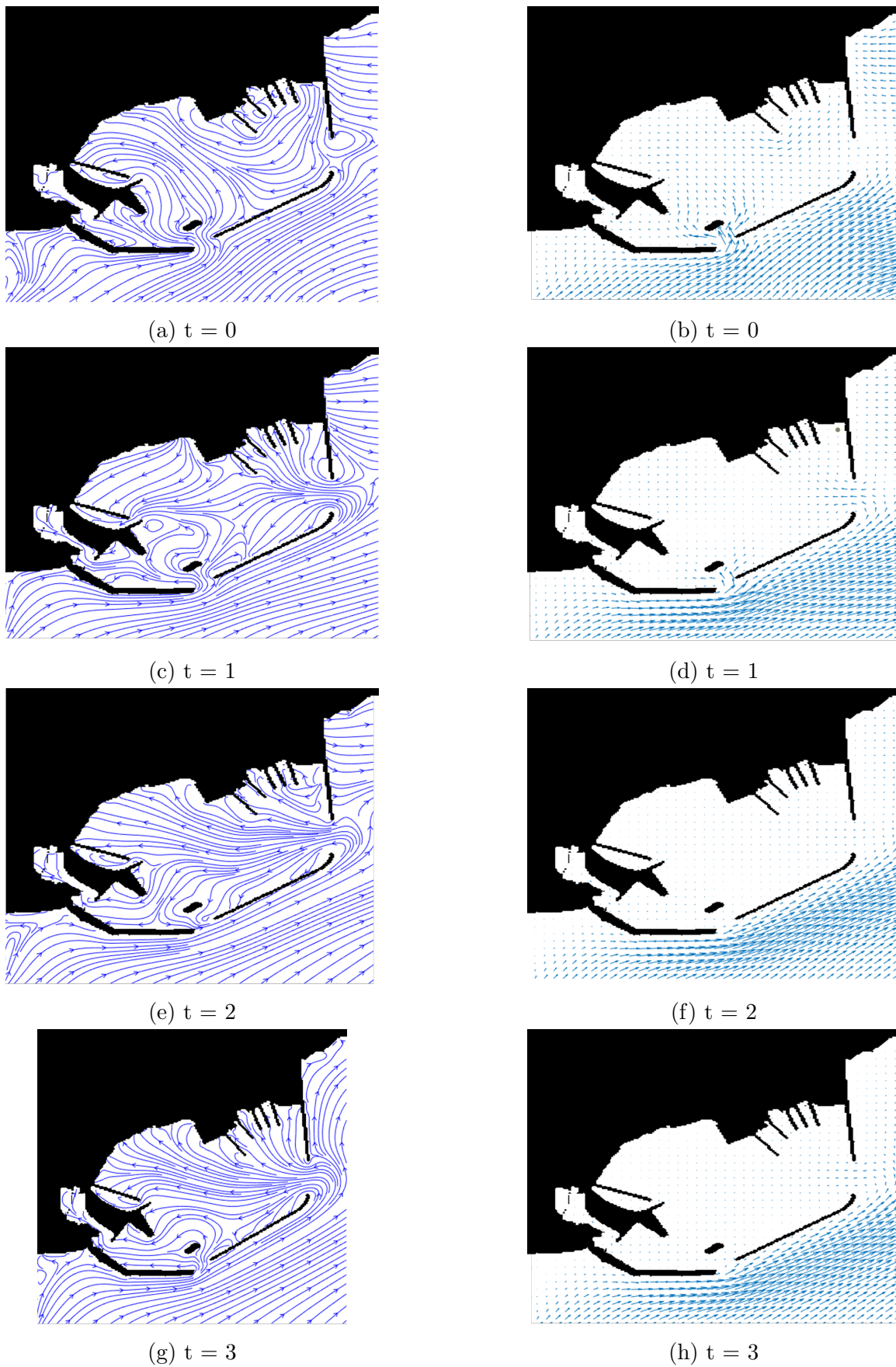


Figure 9: The mean tidal with an extended western harbour breakwater at the opening and a further breakwater within the Outer Harbour area of the western entrance